RSC Advances

ROYAL SOCIETY OF CHEMISTRY

www.rsc.org/advances

Development of cell-laden 3D scaffolds for efficient engineered skin substitutes by collagen gelation

Hyeon Yoon[a, ‡], Ji-Seon Lee [a, ‡], Haejun Yim[b], Geunhyung Kim[c], Wook Chun[a, b, *]

[a] Burn Institute, Hangang Sacred Heart Hospital, College of Medicine, Hallym Univeristy, Youngdeungpu-gu, Seoul 150-719, Korea

[b] Department of Surgery, Hangang Sacred Heart Hospital, College of Medicine, Hallym Univeristy, Youngdeungpu-gu, Seoul 150-719, Korea

[c] Department of Biomechatronic Eng., Sungkyunkwan University (SKKU), Suwon 440-746, South Korea.

[*] Corresponding author (e-mail: chun0414@hallym.ac.kr)

‡ These authors contributed equally to this study.

Keyword

Engineered skin substitute, collagen, gelation, fibroblast, keratinocyte

Abstract

Conventional collagen scaffolds, which were fabricated like spongy types, have been used widely to promote wound repair since they can enhance various cellular activities including cell proliferation and migration, and even guidance of near cells to work as normal tissues functionally. Recently, fabrication technology of 3 dimensional (3D) scaffolds including solid free-form fabrication and rapid prototyping methods is developing from day to day in order to promote wound repair efficiently. In addition, research about constituents, which was filled inside scaffolds, such as a variety of cells, materials and growth factors has been proceeding. In this study, we modified rapid prototyping methods and then set up the cell printing system, which are able to fabricate 3D cell-laden scaffolds for better skin tissue regeneration. These scaffolds are composed of layered structure and were manufactured using collagen, having optimal biocompatibility, and human primary skin cells including epidermal keratinocytes and dermal fibroblasts. Accordingly, these scaffolds are capable of proliferation and migration of keratinocytes and fibroblasts effectively. Therefore, we suggest that these scaffolds can be used as the engineered skin substitute sufficiently.

Introduction

The organ transplantation is the most efficient therapy to treat damaged tissue(s) and organs. Besides, development of autograft, allograft and xenograft of transplantable organs has been progressed. However, organ transplantation has limitations such as immunosuppression after operation as well as lack of donor tissue and organs [1]. For these reasons, many artificial organs have been developed to overcome immunosuppression and demand. And development of these artificial organs was based on tissue engineering, which is multidisciplinary study and whose goal is manufacturing of biological substitutes that replace, maintain or improve their own tissue and organs [2, 3].

Recently, researchers are focusing on the 3 dimensional (3D) scaffolds for generation of artificial organs using synthetic and natural polymers [4, 5]. The structure and properties of 3D scaffolds are very critical and important factors to generate organ. The general requirement of 3D scaffolds are as follows: i) suitable mechanical properties to retain the structure and function for cell proliferation, ii) interconnected pore structure with proper size to infiltrate cell and nutrient, iii) appropriate surface chemistry to promote cell attachment and proliferation. Such scaffolds were used to regenerate bone, vessel, tendon, skin and so on [6-12].

Among various organs, the loss of integument as the largest organ in the human body, can occur by various wounds such as abrasion, bruise, stab, hack, laceration, burn and so on. Especially, thermal trauma is most common skin defect and scalding burn can occur a severe wound rapidly in the wide area and lead to death [13]. Therefore, in case of burn wound healing therapy, the artificial dermis has been used to regenerate defected skin. However, these artificial dermis, including acellular dermal matrix and artificial collagen dermis, have limitations such as high cost, infection derived from donor pathogen, lack of donor tissue,

and secondary autograft skin graft[14]. To overcome these limitations, many researchers have been studied about artificial dermis through various fields including cell biology [15, 16], genetics [17], material engineering [18, 19] and clinical medicine [20, 21]. Furthermore, studies on the scaffolds including cells and cytokines are actively on the way to reduce reconstruction time of wound bed.

These skin wounds can be classified into 4 types; epidermal wound, superficial partial-thickness wound, deep partial-thickness wound and full thickness wound according to increasing depth of the injury [13, 22]. Currently, dressing such as MatriDerm® (Germany), PelnacTM (UK) and Integra (USA) are used extensively to treat skin injury including deep wound or broad skin defect during operation. These dressings, called artificial dermis, were fabricated by conventional methods such as freeze-drying techniques. These artificial dermis consisting of an average thickness of 1 ~ 1.2 mm collagens looks like sponge and are used for efficient re-epithelialization and revascularization on the damaged skin via increase of cell proliferation and migration. However, cell proliferation and migration inside the scaffolds takes a long time to regenerate defected skin. Recently, for this reason, artificial dermis containing cells and growth factors have been researched and applied clinically to reduce the wound healing times [23-26].

Herein, we modified conventional rapid prototyping system and developed novel cell-laden 3D scaffolds including human primary epidermal keratinocytes and dermal fibroblasts by collagen gelation method. These cell-laden scaffolds are composed of 4 layers collagen struts: 1 layer (surface area) as an epidermis containing keratinocytes and other 3 layers (bottom area) as a dermis containing fibroblasts. Besides, these scaffolds are made up of collagen, major component of extracellular matrix, having optimal biocompatibility. Consistently, these 3D scaffolds exhibited noticeably enhanced proliferation *in vitro*.

Therefore, we suggest that these scaffolds can be performed as the engineered skin substitute efficiently.

Materials and methods

Materials

The type I atelo-collagen (Matrixen^{TM}-PSP, Bioland Co., South Korea) was originated from porcine. The DMEM (Dulbecco's Modified Eagle Medium) powder was purchased from Gibco (Cat. No. 12800-017, USA). And other cell culture materials were purchased from Invitrogen (USA).

For cultivation of the keratinocyte and the fibroblast, KGM (keratinocyte growth medium) and FGM (fibroblast growth medium) were purchased from Lonza (USA).

The 3D printing systems

The 3D printing system was composed of 3D robotic system of two parts (DRM60, DRM130 series, Dongburobot, Korea) including a dispensing system (NEP-2000, EST, Korea) and a temperature-controllable stage to move easily at 3 axes. The stage was consisted of 4 parts such as a circulating pump, a temperature controller, water chamber and a manufacturing plate. A sterilized 3rd distilled water was circulated into a plate by circulating pump system to maintain the plate temperature at 25℃ to 60℃. The 3D scaffolds specification was controlled by parameters of 3D plotting system such as a nozzle moving speed, a nozzle tip, and a pneumatic pressure. To fabricate a cell-laden scaffolds, a neutralized collagen solution was placed in the barrel of 3D plotting system. The moving speed of 29G (outer diameter : 340 μm) blunt-end nozzle was fixed at 2 cm/sec and a pneumatic pressure to extrude collagen was fixed at 150 ± 10 kPa.

The collagen solution for fabrication of 3D scaffolds

To fabricate cell-laden 3D scaffolds, porcine type I collagen was used. To make a collagen solution, the collagen powder was dissolved in 0.05 M acetic acid (pH 3.2) at final concentration of 10 % (w/v). The DMEM powder was dissolved in the 100 ml sterilized 3rd distilled water by enrichment up 10 times. A collagen solution and a 10× DMEM were mixed to maintain a neutral pH (pH 7.0) at ratio of 1:1 (v/v). Generally, it is required to neutralize collagen solution essentially since they are acidic (pH 3.2). So, we neutralized acidic collagen solution using 10× DMEM since 10× DMEM contained 3.7g $NaHCO_3$, which was mildly alkaline in aqueous solution due to OH^- group. And 10× DMEM are served as a media to protect and grow cells. These neutralized collagen solution were mixed with cells gently to fabricate cell-printed scaffolds just on the verge of cell printing[27].

Mechanical properties of 3D scaffold

To confirm the mechanical properties, compression test was accomplished. To test compression data, the scaffolds were cut into small strip shapes (5×5 mm^2) and stack up 4 layer. Test was conducted using a tensile instrument (Top-tech 2000; Chemilab, South Korea). The tensile test was performed in a 'wet' state. The stress-strain curves were recorded at a compression speed of 0.5 mm/s. All values are expressed as means ± standard deviation ($n = 3$).

Cell isolation and cultivation

To fabricate cell-laden 3D scaffolds, the primary cells, human epidermal keratinocytes (HEK) and human dermal fibroblasts (HDF), were obtained from MCTT (Modern Cell and Tissue Technologies, Seoul, Korea). Normal HEK and HDF, were isolated from foreskins obtained through routine circumcisions, were cultured as described previously [15, 28, 29]. Briefly, keratinocytes and fibroblasts were isolated from neonatal foreskin obtained through the

clinical circumcisions. The washed foreskin biopsies were cut into the small pieces and incubated in HBSS containing 10mg/ml dispase (Dispase II, Gibco, USA) for 1 hour at 37℃. The epidermis was separated from dermis, and then perturbed by pipetting after incubated in basal medium containing 0.05% trypsin solution for 30 minutes at 37℃ to release keratinocytes. The collected keratinocyte by centrifugation were cultivated in the 100-mm culture dish with keratinocyte growth medium containing the supplementary growth factors. To collect fibroblasts, the dermis were incubated in the PBS containing type II collagenase (Sigma, USA) for 1 hour at 37℃, and fibroblasts were harvested by centrifugation. The harvested fibroblasts were cultured at in the growth medium containing the supplements.

Cell isolation and cultivation for *in vivo* test

To test efficiency of cell-laden 3D scaffolds in *in vivo* mouse model, keratinocytes and fibroblasts were isolated from ICR mouse (HSD:ICR (CD-1®), 1 day, Koatech, Kyunggi, Korea). After peeling off full skin from mouse under the anesthesia with 20 μl anesthetic drugs (zoletil (Virbac, France): rompun (Bayer, Germany) = 1:2), the skin was soaked in the Defined K-SFM (Gibco, USA) including 10% FBS and 1% antibiotics. Then the skin was immersed in PBS including Dispase II (5 mg/ml) and 10% FBS for 1 hour at 37℃ to divide epidermis (keratinocyte) from dermis (fibroblast). To isolate keratinocytes, epidermis was soaked in PBS including 0.25% Trypsin/EDTA for 12 minutes at 37℃. These separated keratinocytes were filtered by 70 μm cell strainer to dissociate single keratinocyte after neutralizing by PBS including 20% FBS. To isolate fibroblasts, dermis was dipped in DMEM including 500 units Collagenase type IV for 1 hour at 37℃ after chopping into small pieces. To neutralize TE buffer, DMEM including 20% FBS was added in media including collagenase. Then, theses seperated fibroblasts were filtered by 70 μm cell strainer.

Scaffolds fabrication condition

First of all, the cell-laden 3D scaffolds were fabricated at the clean bench to maintain an aseptic condition for cell printing techniques. The cell-laden 3D scaffolds were fabricated at two different conditions to confirm the optimal manufacturing process. The pH value of collagen solution was fixed at pH 3, 5, 6, and 7 by 10× DMEM concentration. And plate temperature was set up at 27, 30, 33, 36, 39, 42, 45, and 46 ℃.

Analysis of characteristics

The morphology of cell-laden 3D scaffolds including HDF and HEK was observed under the optical stereomicroscopy (SZ 61, Olympus, Japan) and a laden cell in the scaffolds was confirmed under the inverted microscopy (IX70, Olympus, Japan). And stained scaffolds sections were observed under the optical microscope (DM 750, Leica, Japan).

The mechanical properties of cell-laden 3D scaffolds including HDF and HEK were evaluated by measuring the tensile properties. The scaffolds were cut into small piece (5 × 5 × 1.2 mm) and stack up 4 layers. The uniaxial analysis was carried out using a tensile machine (top-tech 2000, Chemilab, South Korea). To analyze stress-strain curves of cell-laden 3D scaffolds, a moving speed of stretching jig was fixed to at 0.5mm/s.

Live/dead staining

To confirm the viability of printed HDF in the cell-laden 3D scaffolds after cell printing, the cells in a cell-laden 3D scaffolds were exposed to 2μM Calcein AM and 4μM Ethidium homodimer-1 (LIVE/DEAD® Fixable Stains, Life Technologies, USA) for 10 minutes in an incubator in dark conditions. The stained scaffolds were observed under a microscope and the microscopic images were captured by digital camera. A green and red color in the images

indicated live and dead cells, respectively.

Cell proliferation assay

To evaluate cell proliferation of HDF in the cell-laden 3D scaffolds, each scaffolds was analyzed using a MTT cell proliferation assay (sigma, USA). The cells in the scaffolds were merged into 5 mg/ml MTT solution for 4 hours at 37 ℃. Then, an absorbance was detected at 570 nm using multimode reader (DTX 880, Beckman Coulter, USA) after stop reaction using DMSO.

Culture of 3D skin collagen scaffolds

HDF (5×10^5 cells/ 3layer) and HEK (3.2×10^6 cells/ 1layer) were used for fabricating the 3D skin collagen scaffolds. And then air-liquid culture method was performed to evaluate maintenance of cells within the 3D collagen scaffolds. Briefly, the scaffolds were cut into rounds of 8-mm diameter using a biopsy punch, lifted onto an insert grid (140656, Thermo Scientific, Denmark), added to the level of the grid using E-medium (consisting of Dulbecco's modified Eagle's medium and F12 medium in a 3:1 ratio plus 10%

fetal bovine serum, 5 μg/mL insulin, 5 μg/mL transferrin, 2×10^{-8} M T3, 0.1% gentamicin, 10^{-10} M cholera toxin, and 0.4 μg/mL hydrocortisone) and incubated in 5% CO_2 incubator for 7 days. To obtain immunohistochemical data, the scaffolds was cryosectioned with 40 μm-thick and the sections were stained with primary monoclonal antibodies against CK-10 (MA1-06319, Thermo Scientific, Netherlands), vimentin (M0725, Dako, Denmark) for overnight at 4 °C. The slides were then washed in phosphate-buffered saline and incubated with biotinylated horseradish peroxidase–conjugated secondary antibody for 2 hours. and then the slides were washed in phosphate-buffered saline and incubated with streptavidin for 1.5 hours. The sections were incubated in diaminobenzidine (Dako) until the

desired staining intensity was reached. And the slides were counterstained with Fast Red. The sections were also stained with hematoxylin and eosin (H&E) for detection of cell distribution.

Full-thickness excision and grafting in mouse skin

For *in vivo* animal study, ICR mice (female mice, body weight 20-25g, 6 weeks old) were kept in the local animal care facility according to the institution guideline. Twenty mice were included in these experiments. The mice were kept in cage separately in the animal laboratory equipped with controlled condition to optimize animal care. And mice had free access to rodent feed and water ad libitum under the standard laboratory guideline.

Mice were anaesthetized with zoletile/rompun and 1 × 1 cm^2 full-thickness excision of skin was made on the mid back. After injury by excision, mice were randomly divided into five groups of five mice each. Group 1 was non-excision (normal) group as a control. Group 2 was non-treatment group adapted only vaseline gauze dressing after excision by 1 × 1 cm^2. Group 3 and 4 were experimental groups including a 3D scaffolds and vaseline gauze. Group 3 was treated with 3D collagen scaffolds, which were not included HDF and HEK. Group 4 was treated with cell-laden 3D collagen scaffolds, which were included HDF and HEK.

To obtain experimented skin samples, mice were sacrificed in the CO_2 chamber individually. Then the skin was excised including 2 mm margin from experimented area. The excised skin was washed 2 times with PBS to remove blood and dirty particles and then soaked in the 4% paraformaldehyde for 2 days until sufficient permeation. And then, the fixed skin was dipped in 30% sucrose solution including antibiotics for 2 days. To obtain immunohistochemical data, the skin was cryosectioned with 8 μm-thick and stained using haematoxylin and eosin.

This animal study was conducted in accordance with guidelines and approval of the Institutional Animal Care and Use Committees (IACUC) of Hallym University (Hallym-2010-78).

Results and discussion

Overall structure of cell-laden 3D scaffolds

First of all, we confirmed that structure of scaffolds is suitable of 4 layers strut, consisted of 1 keratinocytes layer as a epidermis and 3 fibroblasts layers as a dermis to mimic normal skin tissue (Figure 1A). Therefore, these cell-laden 3D scaffolds (1 keratinocytes layer and 3 fibroblasts layers) are completed by 3D robotic system as shown Figure 1B. The cell-laden 3D scaffolds dimension is 10 mm × 10 mm × 2 mm (W × D × H). A strut and pore size of this scaffolds was measured 300.65 ± 29.35 μm and 294.47 ± 47.08 μm, respectively. And one cell-laden 3D scaffolds contained 5×10^5 cells (fibroblasts) and 3.6×10^6 cells (keratinocytes).

Temperature optimization of cell-laden 3D scaffolds

Next, cell-laden 3D scaffolds were manufactured under various conditions, such as different temperature and pH to confirm an optimal condition of fabrication. First of all, we tried to optimize temperature for fabrication of cell-laden 3D scaffolds. The morphology of temperature-dependent scaffolds is as shown Figure 2A. To analyze morphology of scaffolds, a strut of the scaffolds was fabricated as one layer. As a result, the optimal temperature of scaffolds fabrication is between 36 and 39 ℃. In case of 37 ℃ of plate temperature, strut size and pore structure inside scaffolds were uniform than other temperature condition. Whereas, the collagen scaffolds was not fabricated totally below 36 ℃ or over 46 ℃. In addition, collagen strut spreads out on the plate widely when temperature range of plate is out of the optimal condition (27 - 33 ℃, 42 - 45 ℃), and these spread-out strut of scaffolds cannot form sufficient uniformed pore size for cell proliferation eventually. In the previous study, neutralized collagen solution formed fiber at 35 ~ 40℃ quickly. On the other hand,

neutralized collagen solution was not able to form a strut under the ~ 35℃, because collagen fibrillation was processed slowly under ~ 35℃ [30-34]. Also in our result, the neutralized collagen solution was turned into water and cannot form a strut over 42℃. This phenomenon surmised that neutralized collagen was denatured under high temperature condition.

Uniform diameter distribution of strut is also a considerable factor when the struts in the scaffolds were printed on the temperature-controllable stage at variety of temperature to confirm optimal gelation temperature condition of neutralized collagen solutions. As the plate temperature increased from 27 to 39 ℃, a strut size was decreased to 300 μm. And also in case of temperature from 27 to 33 ℃, size distribution was too broader since temperature of collagen gelation is not sufficiently high. Finally, the strut of scaffolds was spread out on the plate and the scaffolds were not manufactured to adequate structure. On the other hand, in case of 45 ℃, the strut was not spread adequately compared with temperature below 36 ℃ although the strut size was about 300 μm (Figure 2B).

Moreover, a strut size was noticeably the smallest in fabrication conditions at 39 ℃ (Figure 2C, D). These results revealed that stage temperature of a collagen gelation is optimal to 39 ℃ to fabricate cell-laden 3D scaffolds.

pH optimization of cell-laden 3D scaffolds

Collagen gelation depends on condition of pH as well as temperature. Therefore, we tried to fabricate cell-laden 3D scaffolds in pH-dependent manner to find out optimal pH. Figure 3 shows morphology of collagen scaffolds, which were fabricated at different pH levels as 3, 5, 6, and 7. In case of pH 3, a strut of collagen scaffolds was not maintained uniformly and retained pore structure and adequate 3D structure for proper cell proliferation

and migration. At pH 5 and 6, the scaffolds cannot be used for skin regeneration due to their swollen strut since primary human skin cells such as keratinocyte and fibroblast cannot live in acidic environment. As anticipated, the scaffolds were fabricated adequately to regenerate damaged skin when a collagen solution was at pH 7. And this condition provided a cell viable environment.

Mechanical properties of cell-laden 3D scaffolds

The mechanical properties of scaffolds are very important element to organ transplantation [35]. To adapt cell-laden 3D scaffolds into clinical field, these scaffolds should have porous structure not only with good biocompatibility but also with high mechanical strength [36]. Therefore, we carried out an analysis of mechanical properties using universal tensile machine in order to confirm mechanical properties of cell-laden 3D scaffolds, which was fabricated including a keratinocyte and fibroblast in the 4 layers at 37℃. As a result, value of young's moduli of scaffolds is 0.01 ± 0.001 KPa as young's moduli of scaffolds were measured by tensile machine (Figure 4). Generally, the young's modulus of scaffolds is low since scaffolds were not cross-linked. However, it is necessary to increase the strength for clinical applications. Therefore, the following procedure is to enhance the strength using a cross-linking reagent of the scaffolds.

Characteristics of cells inside cell-laden 3D scaffolds

In general, cell viability was decreased during cell printing process as cells were extruded from nozzle due to a shear stress [37]. First of all, we carried out live/dead cell staining to confirm that cells inside scaffolds retained their properties after 3D cell printing through collagen gelation methods. In Figure 5A, these scaffolds were fabricated 1 layer including fibroblast and then were immunostained with Calcein AM (green, live cells) and

Ethidium homodimer-1 (red, dead cells). As a result, the ratio of the live and dead cells was 84.9% and 15.1%, respectively. Therefore, this condition (from 36 to 39 ℃) is proper temperature to survive cells whereas cell viability was significantly decreased over the 39 ℃ [38].

And then, we tested proliferation assay using MTT solution to confirm that cells inside cell-laden 3D scaffolds can proliferate properly (Figure 5B). The scaffolds were fabricated to three layers including only 5 $\times 10^5$ cell of fibroblasts. And the control group was used to culture the cells on the TCP (tissue culture plate). After 1, 3 and 7 days, each scaffolds were soaked in the MTT assay solution for 4 hours and then a DMSO was added to stop the reaction according to direction of MTT assay. As a result, in the 3D cell-laden scaffolds, cells are marginally increased in a time-dependent manner. But, the cells of control group were cultured in the 6 well plate. After 3 days, proliferation rate was not increased. This reason is that a space which to grow was lack. Therefore, cell-laden 3D scaffold was provided an efficient and enough space to skin regeneration.

Moreover, cell-laden 3D scaffolds have capability of release and migration of the cells inside scaffolds strut. Therefore, we observed release and migration of cells inside scaffolds strut in time-dependent manner. Cells inside strut released initially after 5 days of scaffolds fabrication. And then the released cells were attached, proliferated and migrated into cell culture plate. According to analysis of image J, these cells were confluent over 95% after 36 days. Therefore, these data indicated that cells inside scaffolds are sufficient to release scaffolds out and proliferate.

Distribution of cells including keratinocytes and fibroblasts is a key factor in order that cell-laden 3D scaffolds are used as engineered skin substitute efficiently. Therefore, the cell-

laden 3D scaffolds were maintained through air-liquid culture methods and stained with CK-10 and vimentin, which is specific marker for keratinocytes and fibroblasts, respectively. Keratinocytes inside scaffolds are mostly distributed in surface area regarding as an epidermis and fibroblasts inside scaffolds are well dispersed in bottom area regarding as a dermis (Figure 5D). Accordingly, these data indicated that each skin cells maintain their own location despite over time. In other words, cell location can be controlled to regenerate damaged skin during fabrication of cell-laden 3D scaffolds. Besides, these cells in the scaffolds can be not only keep a dermal and epidermal layer but also release and proliferate into the wound bed.

Efficiency of cell-laden 3D scaffolds in *in vivo* animal model

In figure 6 shows an operation process (a) and immunohistochemistry data (b). Cell-laden 3D scaffolds were located on the wound bed, which was excision site on the mouse mid back (Figure 6A). Then wound dressing was covered on the scaffolds using vaseline gauze. After 1 week, damaged skin samples are immunostained with haematoxylin and eosin. As a result, group 3 and 4 was quickly and almost perfectly repaired, compared with group 2. The damaged skin was regenerated almost completely and clearly. Also hair follicle was regenerated almost perfectly on the wound bed. However, group 3 and 4 were not dramatically different. We speculated that scaffolds promoted skin regeneration since scaffolds are consisted of collagen, but the time of cell release from scaffolds was not enough. Thus two weeks or longer might be required to confirm a satisfactory effect.

Conclusions

Herein, we tried to develop cell-laden 3D scaffolds, which can be used for better regeneration of damaged skin. Therefore, we presented collagen scaffolds consisting collagen

and human primary skin cells including keratinocytes and fibroblasts by 3D cell printing systems. Our cell-laden 3D scaffolds are well-designed for skin regeneration since collagen, major component of extracellular matrix, have outstanding biocompatibility and cells inside scaffolds were constituted as a cell-laden layered structure to mimic human normal skin. Besides, skin cells inside scaffolds are certificated since these cells-containing cell therapy products are sold commercially as a cultured epithelial autograph (CEA). Moreover, the keratinocytes and fibroblasts are dispersed within the scaffolds properly for efficient skin regeneration. However, our cell-laden 3D scaffolds are not used as an engineered skin substitute (ESS) commercially since scaffolds are difficult to handle due to lower stiffness facto in spite of sufficient efficiency for wound healing. Currently we are trying to increase strength and stiffness by crosslinking cell-laden 3D scaffolds using non-toxic chemical reagent such as genipin[39-42]. Therefore, the developed cell-laden 3D scaffolds using non-toxic chemical reagent, enhance their strength and then carry out *in vivo* study again to be used as ESS effectively in the future.

Acknowledgement

This study was supported by a grant of the Korean Health Technology R&D Project, Ministry of Health & Welfare, Republic of Korea. (A 120942)

References

1. A. S. Chong and M. L. Alegre, *Nature reviews. Immunology*, 2012, **12**, 459-471.
2. R. Shalak and C. Fox, *Tissue Engineering*, 1988, 26-29.
3. E. Sachlos and J. T. Czernuszka, *Eur Cell Mater*, 2003, **5**, 29-39.
4. J. Y. Lee, B. Choi, B. Wu and M. Lee, *Biofabrication*, 2013, **5**, 045003.

5. T. Xu, K. W. Binder, M. Z. Albanna, D. Dice, W. Zhao, J. J. Yoo and A. Atala, *Biofabrication*, 2013, **5**, 015001.
6. Q. Lu, K. Ganesan, D. T. Simionescu and N. R. Vyavahare, *Biomaterials*, 2004, **25**, 5227-5237.
7. S. Yang, K. F. Leong, Z. Du and C. K. Chua, *Tissue Eng*, 2001, **7**, 679-689.
8. U. J. Kim, J. Park, H. J. Kim, M. Wada and D. L. Kaplan, *Biomaterials*, 2005, **26**, 2775-2785.
9. C. M. Agrawal and R. B. Ray, *J Biomed Mater Res*, 2001, **55**, 141-150.
10. J. O. Hollinger and K. Leong, *Biomaterials*, 1996, **17**, 187-194.
11. R. Augustine, E. A. Dominic, I. Reju, B. Kaimal, N. Kalarikkal and S. Thomas, *RSC Advances*, 2014, **4**, 24777-24785.
12. N. Bhardwaj, W. T. Sow, D. Devi, K. W. Ng, B. B. Mandal and N.-J. Cho, *Integrative Biology*, 2015, **7**, 53-63.
13. R. V. Shevchenko, S. L. James and S. E. James, *Journal of the Royal Society, Interface / the Royal Society*, 2010, **7**, 229-258.
14. G. Guan, L. Bai, B. Zuo, M. Li, Z. Wu, Y. Li and L. Wang, *Bio-medical materials and engineering*, 2010, **20**, 295-308.
15. S. Ahn, H. Yoon, G. Kim, Y. Kim, S. Lee and W. Chun, *Tissue engineering. Part C, Methods*, 2010, **16**, 813-820.
16. H. J. You and S. K. Han, *Journal of Korean medical science*, 2014, **29**, 311-319.
17. S. Park, J. I. Kim, I. Lee, J. Y. Bae, M. W. Hwang, D. Kim, S. I. Jang, H. Kim, M. S. Park, H. J. Kwon, J. W. Song, Y. S. Cho, W. Chun and M. S. Park, *BMC microbiology*, 2014, **14**, 237-245.
18. N. Kanda, N. Morimoto, S. Takemoto, A. A. Ayvazyan, K. Kawai, Y. Sakamoto, T. Taira and S. Suzuki, *Annals of plastic surgery*, 2012, **69**, 569-574.
19. S. A. Muller, A. van der Smissen, M. von Feilitzsch, U. Anderegg, S. Kalkhof and M. von Bergen, *J Mater Sci Mater Med*, 2012, **23**, 3053-3065.
20. N. Morimoto, K. Yoshimura, M. Niimi, T. Ito, R. Aya, J. Fujitaka, H. Tada, S. Teramukai, T. Murayama, C. Toyooka, K. Miura, S. Takemoto, N. Kanda, K. Kawai, M. Yokode, A. Shimizu and S. Suzuki, *Tissue engineering. Part A*, 2013, **19**, 1931-1940.
21. L. Troisi, G. Papa, V. Ramella and Z. M. Arnez, *Journal of tissue viability*, 2015, DOI: 10.1016/j.jtv.2015.07.001.

22. R. Papini, *Bmj*, 2004, **329**, 158-160.
23. N. Morimoto, N. Kakudo, P. Valentin Notodihardjo, S. Suzuki and K. Kusumoto, *Journal of artificial organs : the official journal of the Japanese Society for Artificial Organs*, 2014, **17**, 352-357.
24. M. Ehrenreich and Z. Ruszczak, *Tissue Eng*, 2006, **12**, 2407-2424.
25. A. Langer and W. Rogowski, *BMC Health Serv Res*, 2009, **9**, 115.
26. H. Uchi, A. Igarashi, K. Urabe, T. Koga, J. Nakayama, R. Kawamori, K. Tamaki, H. Hirakata, T. Ohura and M. Furue, *European journal of dermatology : EJD*, 2009, **19**, 461-468.
27. Y. Song, M. Zhang, L. Zhao, X. Yin, J. Zhao, J. Li, R. He, Y. Chang, J. Jin and Y. Zhao, *Nanomedicine: Nanotechnology, Biology and Medicine*, 2014, **10**, 783-793.
28. H. Green, O. Kehinde and J. Thomas, *Proceedings of the National Academy of Sciences of the United States of America*, 1979, **76**, 5665-5668.
29. L. Pirisi, S. Yasumoto, M. Feller, J. Doniger and J. A. DiPaolo, *Journal of virology*, 1987, **61**, 1061-1066.
30. M. D. Brigham, Massachusetts Institute of Technology, 2007.
31. J. M. Menter, A. M. Patta, R. M. Sayre, J. Dowdy and I. Willis, *Photodermatology, photoimmunology & photomedicine*, 2001, **17**, 114-120.
32. C. Mu, D. Li, W. Lin, Y. Ding and G. Zhang, *Biopolymers*, 2007, **86**, 282-287.
33. A. W. Pederson, J. W. Ruberti and P. B. Messersmith, *Biomaterials*, 2003, **24**, 4881-4890.
34. J. Rosenblatt, B. Devereux and D. Wallace, *Biomaterials*, 1994, **15**, 985-995.
35. J. L. Drury and D. J. Mooney, *Biomaterials*, 2003, **24**, 4337-4351.
36. T. Uemura, J. Dong, Y. Wang, H. Kojima, T. Saito, D. Iejima, M. Kikuchi, J. Tanaka and T. Tateishi, *Biomaterials*, 2003, **24**, 2277-2286.
37. N. E. Fedorovich, J. R. De Wijn, A. J. Verbout, J. Alblas and W. J. Dhert, *Tissue engineering. Part A*, 2008, **14**, 127-133.
38. L. E. Gerweck, *Radiation research*, 1977, **70**, 224-235.
39. A. Bigi, G. Cojazzi, S. Panzavolta, N. Roveri and K. Rubini, *Biomaterials*, 2002, **23**, 4827-4832.
40. Y.-F. Michael F. Butler, Paul D.A. Paul D.A. Pudney., *Journal of Polymer Science: Part A: Polymer Chemistry*, 2003, **41**, 1745–1869.
41. H. W. Sung, W. H. Chang, C. Y. Ma and M. H. Lee, *Journal of biomedical materials*

research. Part A, 2003, **64**, 427-438.

42. G. Fessel, J. Cadby, S. Wunderli, R. van Weeren and J. G. Snedeker, *Acta Biomater*, 2014, **10**, 1897-1906.

Figure Legends

Figure 1. **Overall structure of cell-laden 3D scaffolds** A. A scheme of cell-laden 3D scaffolds, consisted of 1 layer (surface area) with keratinocytes and the other 3 layers (bottom area) with keratinocytes by cell printing techniques. B. Morphology of fabricated collagen cell-laden 3D scaffolds.

Figure 2. **Temperature-dependent cell-laden 3D scaffolds** A. Morphology of one-layer cell-laden 3D scaffolds, which were fabricated on different temperature condition without cell. B. Strut size distribution of cell-laden 3D scaffolds at various temperature conditions. C. Diameter of cell-laden 3D scaffolds struts, fabricated with a different temperature of plate. D. Table of relationship between temperature and the diameter

Figure 3. **pH-dependent cell-laden 3D scaffolds** Morphology of one-layer cell-laden 3D scaffolds dependent on different pH of collagen solutions.

Figure 4. **Strength of cell-laden 3D scaffolds** Young's moduli of 3D cell-laden scaffolds under wet condition.

Figure 5. **Activity of cells inside cell-laden 3D scaffolds** A. The images of a Live / Dead cell staining after one-layer cell printing with HDF (×200). Cell-laden scaffolds are soaked in the PBS including 2mM Calcein AM and 4mM Ethidium homodimer-1. B. MTT assay of cell-laden scaffolds using a fibroblast after 1, 3, 7 days of cell printing. * is $P < 0.005$ and ** is $P < 0.001$ C. The images of cell released and migrated from scaffolds after 5, 10, 15, 36 days of fabrication (×100) D. The immunohistochemical images of 3D cell-laden scaffolds through air liquid culture. Each section was stained with H&E, CK-10 and vimentin for location of fibroblast and keratinocytes.

Figure 6. **Efficiency of cell-laden 3D scaffolds in full-thickness excision mouse model** A. The process of experiment for full-thickness excision and cell-laden 3D scaffolds grafting B. H&E staining images of (a) normal skin (b) only full-thickness excised skin (c) full-thickness excised and only 3D scaffolds without cells grafted skin (d) full-thickness excised and only 3D scaffolds with cells grafted skin one week after operation

Figure 1

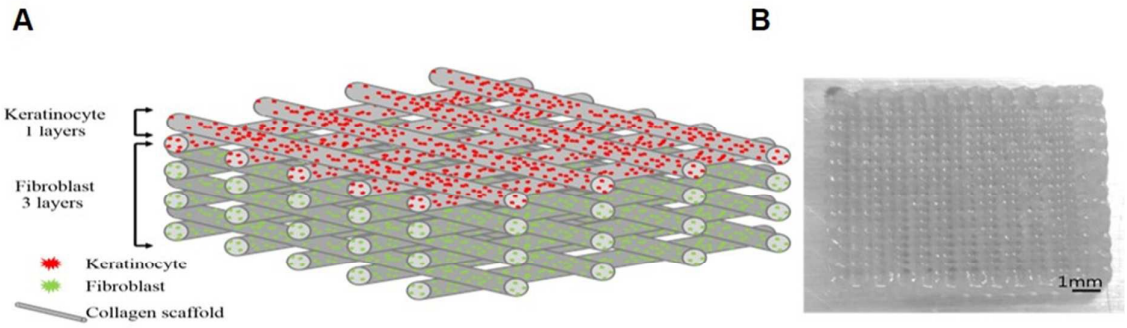

Figure 2

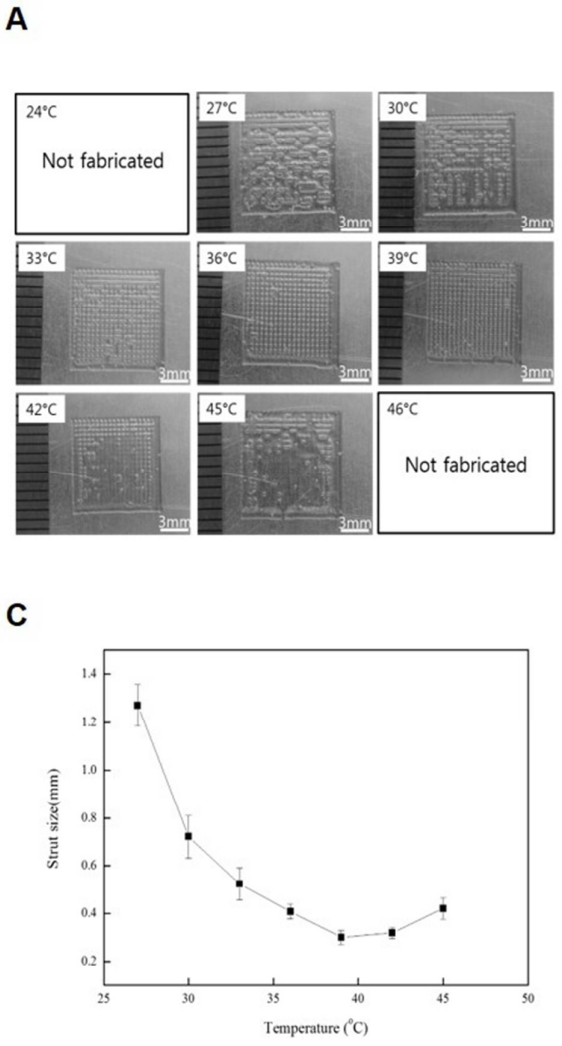

Temperature of Plate (℃)	27	30	33	36	**39**	40	41	42	45
average strut size (um)	1271.86	757.57	523.56	408.24	**300.66**	317.96	394.55	318.91	420.47
standard deviation (um)	86.54	89.57	67.41	30.73	**29.35**	26.80	48.12	23.69	44.20

Figure 3

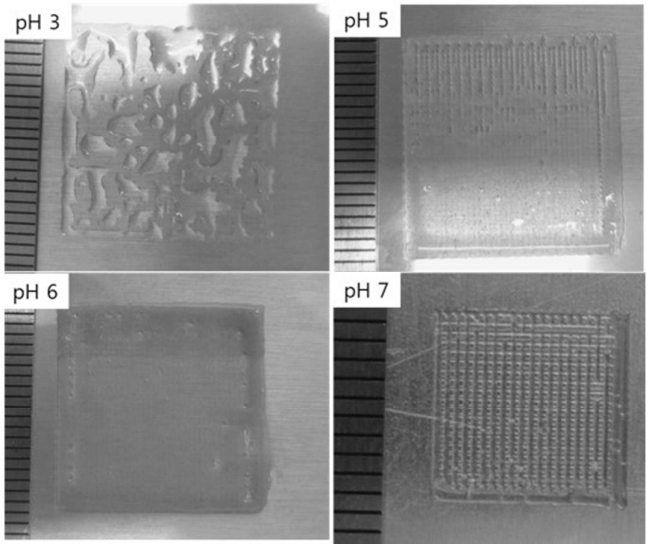

Figure 4

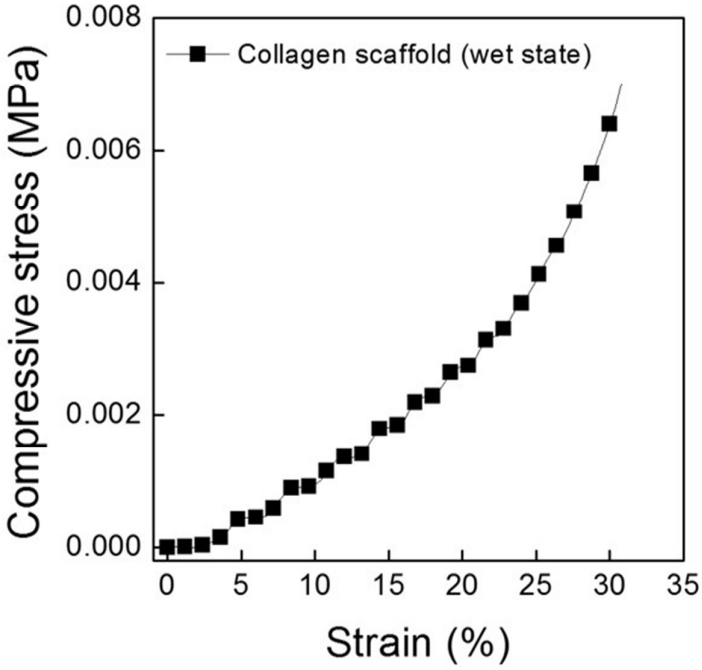

Figure 5

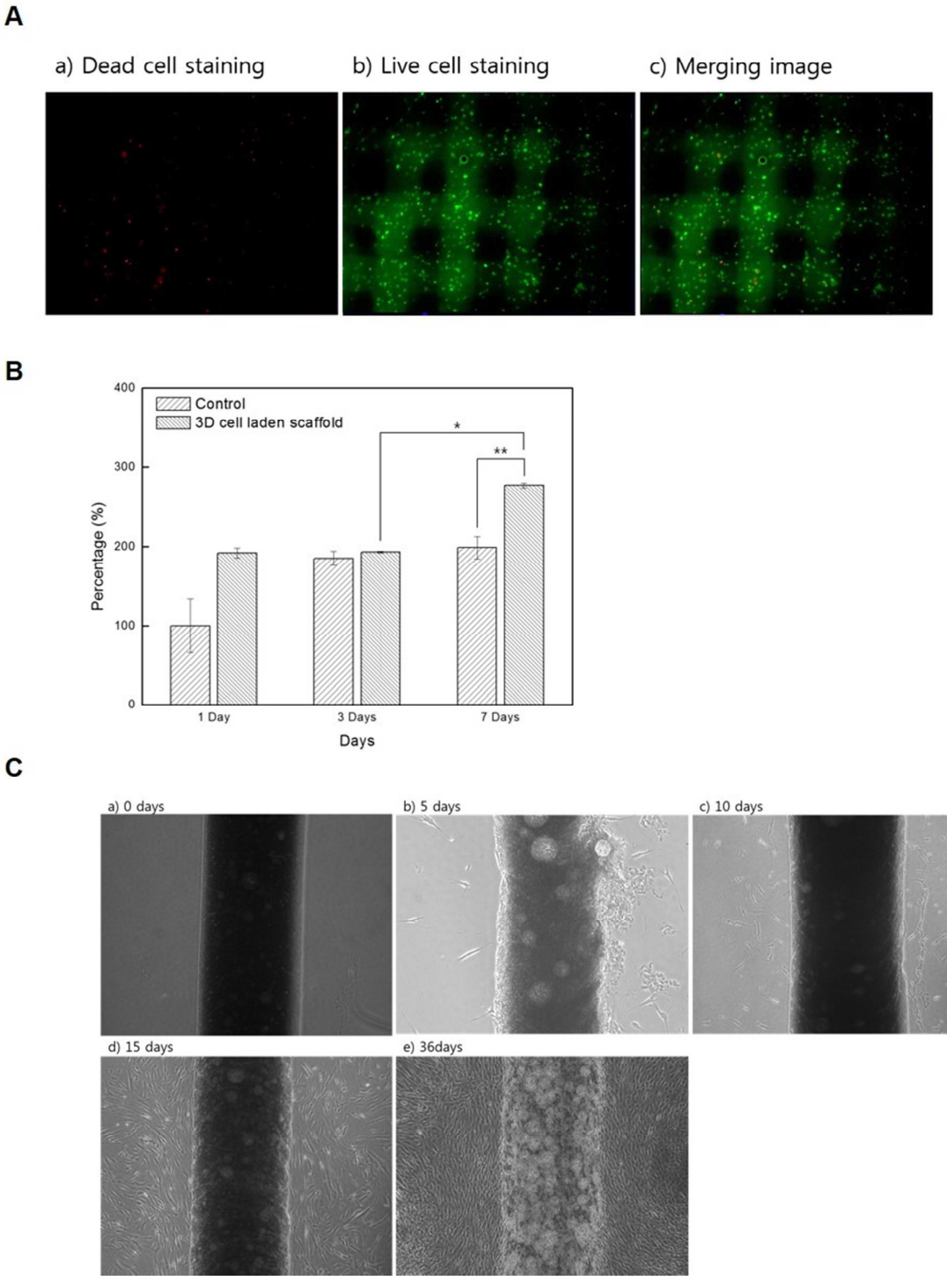

Figure 5

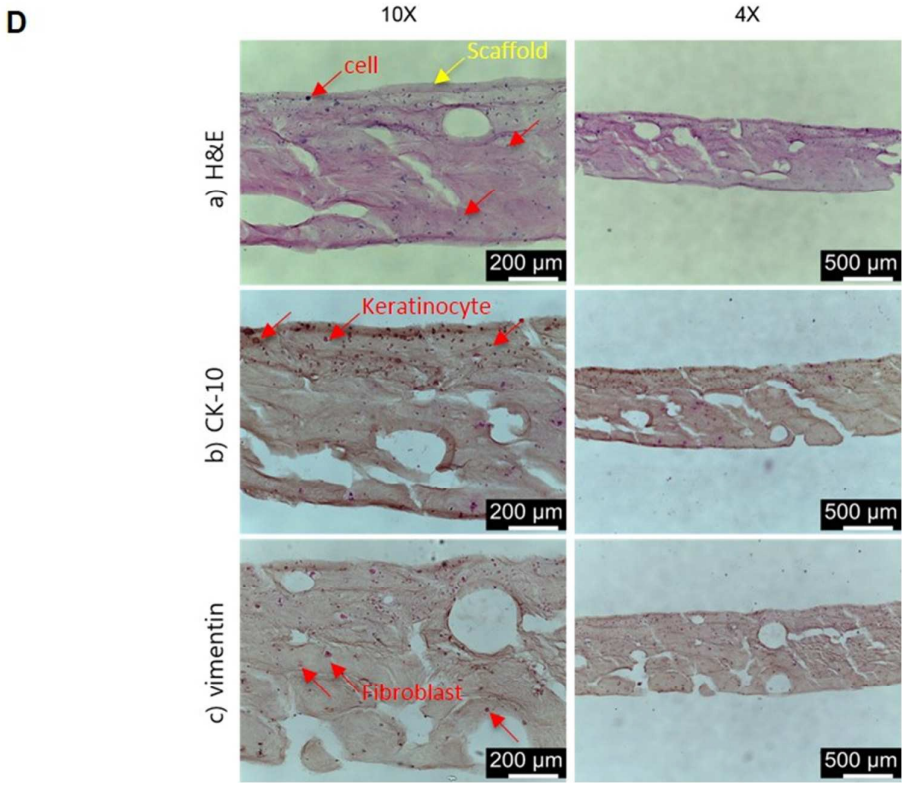

Figure 6